Preparation and Structure of Compounds Containing the $[Rh_2X_7(PR_3)_2]^-$ Anion and Their Stereospecific Reactions with Phosphines To Produce $[Rh_2X_7(PR_3)_3]^-$ Species

F. Albert Cotton* and Seong-Joo Kang

Department of Chemistry and Laboratory for Molecular Structure and Bonding, Texas A&M University, College Station, Texas 77843

Received November 6, 1992

The preparation and characterization of the face-sharing bioctahedral anions $[Rh_2X_7(PEt_3)_2]^-$ (X = Cl, Br) as well as their reactions with additional phosphine (PMe_3, PEt_3, PMe_2Ph) are reported. Reactions with 1 mol of added phosphine leads stereospecifically to one isomer of an edge-sharing bioctahedral species, $[1,6,8\text{-}Rh_2X_7(PR_3)_3]^-$. A solution of $[NEt_4][1,5\text{-}Rh_2Br_7(PEt_3)_2]$ to which 1 molar equiv of PEt_3 has been added at −20 °C reaches an equilibrium in which $[1,5\text{-}Rh_2Br_7(PEt_3)_2]^-$, $[1,6,8\text{-}Rh_2Br_7(PEt_3)_3]^-$, 1,2,6-$Rh_2Br_6(PEt_3)_3$ and [*trans*-$RhBr_4(PEt_3)_2]^-$ are all present. All reactions in solution were monitored by $^{31}P\{^1H\}$ NMR spectroscopy, which, in every case, showed clean, stereospecific reactions. X-ray crystallography was used, as necessary, to support or elucidate structural assignments implied by the NMR spectra. Four crystal structures are presented: $[PPh_4][1,5\text{-}Rh_2Cl_7(PEt_3)_2]$ (**1**), space group $P2_1/c$, a = 16.959(4) Å, b = 9.469(2) Å, c = 26.826(3) Å, β = 91.38(1)°, V = 4306(1) Å^3, Z = 4; $[PPh_4][1,6,8\text{-}Rh_2Cl_7(PEt_3)_2(PMe_3)]$ (**2**); space group $P2_1/n$, a = 10.969(1) Å, b = 17.245(4) Å, c = 25.438(6) Å, β = 93.31(1)°, V = 4804(2) Å^3, Z = 4; $[NEt_4][1,5\text{-}Rh_2Br_7(PEt_3)_2]$ (**3a**), space group, $P\bar{1}$, a = 17.368(3) Å, b = 17.872(3) Å, c = 12.306(3) Å, α = 90.99(5)°, β = 98.84(3)°, γ = 72.82(6)°, V = 3603(1) Å^3, Z = 2; $[PPh_4][$*trans*-$RhCl_4(PEt_3)_2]$ (**4**), space group $P2_1/n$, a = 12.229(1) Å, b = 17.809(3) Å, c = 18.506(4) Å, β = 103.39(1)°, V = 3921(1) Å^3, Z = 4.

Introduction

From earlier work in this laboratory[1,2] it is known that transformations of the type shown in eq 1 proceed easily, reversibly,

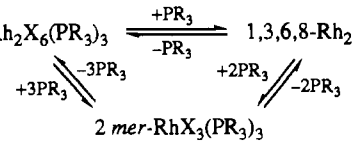

(1)

and with complete stereospecificity. We have now extended our work to cover the chemistry of the related compounds of $[Rh_2X_7(PR_3)_2]^-$ and species obtainable therefrom by reactions with more phosphine. Neither the anions of this kind nor the $[Rh_2X_7(PR_3)_3]^-$ anions that can be obtained from them have previously been described.

In this paper we report the preparation and the crystallographic characterization of the new compounds $[PPh_4][1,5\text{-}Rh_2Cl_7(PEt_3)_2]$ (**1**), $[PPh_4][1,6,8\text{-}Rh_2Cl_7(PEt_3)_2(PMe_3)]$ (**2**), $[NEt_4][1,5\text{-}Rh_2Br_7(PEt_3)_2]$ (**3a**), and $[PPh_4][$*trans*-$RhCl_4(PEt_3)_2]$ (**4**) and studies by $^{31}P\{^1H\}$ NMR spectroscopy of the way in which the reactions shown in eq 2 proceed.

$$[1,5\text{-}Rh_2X_7(PR_3)_2]^- \xrightarrow{+PR_3} [1,6,8\text{-}Rh_2X_7(PR_3)_3]^- \xrightarrow{+2PR_3} [t\text{-}RhX_4(PR_3)_2]^- + mer\text{-}RhX_3(PR_3)_3 \quad (2)$$

Experimental Section

Preparative Procedures. General Procedures. All operations were performed under an atmosphere of argon with carefully dried and distilled solvents by using standard Schlenk line techniques. The $^{31}P\{^1H\}$ NMR spectra were recorded on a Varian XL-200 operating at 81 MHz in 10-mm NMR tubes. Chemical shifts were referenced to an external standard of 85% phosphoric acid.

Starting Material. $RhCl_3\cdot 3H_2O$ and $RhBr_3\cdot 2H_2O$ were purchased from Aldrich or Sigma Chemical Co. PMe_3, PMe_2Ph, and PEt_3 (Strem Chemicals) were transferred into Schlenk tubes and kept under argon. These were stored in the refrigerator when not in use. The compounds 1,2,6-$Rh_2X_6(PEt_3)_3$ (X = Cl, Br) were prepared as previously described.[1]

$[PPh_4][1,5\text{-}Rh_2Cl_7(PEt_3)_2]$ (1). 1,2,6-$Rh_2Cl_6(PEt_3)_3$ (0.55 g, 0.71 mmol) and slightly more than 1 molar equiv of PPh_4Cl (0.32 g; 0.84 mmol) were refluxed in 10 mL of 1,4-dichlorobutane for 1 day. The volume was reduced to about 2 mL and hexane was added. The resulting precipitate was washed with hexane, followed by a small amount of methanol, and then dried in vacuum. Yield: 0.57 g (78%). Red crystals suitable for X-ray crystallographic analysis were obtained by slow diffusion of hexane into an acetone solution of $[PPh_4][1,5\text{-}Rh_2Cl_7(PEt_3)_2]$. $^{31}P\{^1H\}$ NMR: δ 60.0 (d, 2P, J = 116 Hz), 29.9 (s, 1P).

Reaction between 1 and PR_3 (1 equiv; PR_3 = PEt_3, PMe_3, and PMe_2Ph). Formation of Edge-Sharing $[PPh_4][1,6,8\text{-}Rh_2Cl_7(PEt_3)_2(PR_3)]$ Complexes. An acetone solution of 1 was prepared at room temperature, transferred to a NMR tube, and purged with argon. After the solution was cooled to −30 °C, 1 equiv of a tertiary phosphine was introduced with a microsyringe. The reaction appeared to be complete immediately after the addition of the tertiary phosphine. Hexane was added to obtain a precipitate. $^{31}P\{^1H\}$ NMR: $[PPh_4][1,6,8\text{-}Rh_2Cl_7(PEt_3)_3]$, δ 56.6 (d, 1P, J = 115 Hz), 29.9 (s, 1P), 15.3 (d, 2P, J = 81 Hz); $[PPh_4][1,6,8\text{-}Rh_2Cl_7(PEt_3)_2(PMe_3)]$, δ 56.3 (d, 1P, J = 116 Hz), 30.0 (s, 1P), 10 (4d, 2P, $J_{P\text{-}P',trans}$ = 633 Hz, J = 82 Hz); $[PPh_4][1,6,8\text{-}Rh_2Cl_7(PEt_3)_2(PMe_2Ph)]$, δ 56.6 (d, 1P, J = 116 Hz), 30.0 (s, 1P), 10 (4d, 2P, $J_{P\text{-}P',trans}$ = 624 Hz, J = 85 Hz). Red crystals suitable for X-ray crystallographic analysis were obtained by slow diffusion of hexane into an acetone solution of $[PPh_4][1,6,8\text{-}Rh_2Cl_7(PEt_3)_2(PMe_3)]$ (**2**) at −20 °C.

Reaction of $[PPh_4][1,6,8\text{-}Rh_2Cl_7(PEt_3)_3]$ with PEt_3. Formation of *mer*-$RhCl_3(PEt_3)_3$ and $[PPh_4][$*trans*-$RhCl_4(PEt_3)_2]$. An acetone solution of $[PPh_4][1,6,8\text{-}Rh_2Cl_7(PEt_3)_3]$ was prepared at room temperature, transferred to a NMR tube, and purged with argon. To this solution was introduced 3 equiv of triethylphosphine with a microsyringe. The resulting solution was monitored by $^{31}P\{^1H\}$ NMR spectroscopy. $^{31}P\{^1H\}$ NMR: *mer*-$RhCl_3(PEt_3)_3$, δ 26.8 (2t, 1P, J = 112 Hz, $J_{P\text{-}P,cis}$ = 24 Hz), 11.0 (2d, 2P, J = 84 Hz, $J_{P\text{-}P,cis}$ = 24 Hz); $[PPh_4][$*trans*-$RhCl_4(PEt_3)_2]$, δ 12.9 (1d, 2P, J = 84 Hz), 30.0 (s, 1P).

$[Y][1,5\text{-}Rh_2Br_7(PEt_3)_2]$ (Y = NEt_4 (3a), PPh_4 (3b)). 1,2,6-$Rh_2Br_6(PEt_3)_3$ (0.100 g; 0.10 mmol) and slightly more than 1 equiv of NEt_4Br or PPh_4Br were refluxed in 15 mL of 1,2-dibromoethane for 8 h. The volume of the solution was reduced to about 2 mL, and hexane was

(1) Cotton, F. A.; Kang, S.-J.; Mandal, S. K. *Inorg. Chim. Acta* **1992**, *206*, 29.
(2) Cotton, F. A.; Eglin, J. L.; Kang, S.-J. *Inorg. Chem.*, preceding paper in this issue.

0020-1669/93/1332-2336$04.00/0

Table I. Crystallographic Data for **1**, **2**, **3a**, and **4**

	1	2	3a	4
formula	$Rh_2Cl_7P_3C_{36}H_{50}$	$Rh_2Cl_7P_4C_{39}H_{59}$	$Rh_2Br_7P_2NC_{20}H_{50}$	$RhCl_5P_3C_{36}H_{50}$
fw	1029.70	1105.78	1131.76	820.44
space group	$P2_1/c$ (No. 14)	$P2_1/n$ (No. 14)	$P\bar{1}$ (No. 2)	$P2_1/n$ (No. 14)
a, Å	16.959(4)	10.969(1)	17.368(3)	12.229(1)
b, Å	9.469(2)	17.245(4)	17.872(3)	17.809(3)
c, Å	26.826(3)	25.438(6)	12.306(3)	18.506(4)
α, deg	90	90	90.99(5)	90
β, deg	91.38(1)	93.31(1)	98.84(3)	103.39(1)
γ, deg	90	90	72.82(6)	90
V, Å^3	4306(1)	4804(2)	3603(1)	3921(1)
Z	4	4	4	4
d_{calc} g/cm^3	1.59	1.53	2.086	1.39
μ, cm^{-1}	13.29	12.23	86.96	8.48
λ, Å	0.710 73	0.710 73	0.710 73	0.710 73
temp, °C	20 ± 1	20 ± 1	20 ± 1	20 ± 1
transm factors	0.99–0.81	0.99–0.94	0.99–0.73	0.99–0.96
R^a	0.042	0.0436	0.0548	0.0452
$R_w{}^b$	0.0618	0.0652	0.0678	0.0702

^{a} $R = \sum||F_o| - |F_c||/\sum|F_o|$. ^{b} $R_w = [\sum w(|F_o| - |F_c|)^2/\sum w|F_o|^2]^{1/2}$; $w = 1/\sigma^2\{|F_o|\}$.

added. The brown precipitate was washed with hexane, followed by a small amount of methanol and then dried in vacuum. Yield: 0.05 g (50%). Brown crystals of $[NEt_4][1,5\text{-}Rh_2Br_7(PEt_3)_2]$ (**3a**) suitable for X-ray diffractometry were obtained by slow diffusion of hexane into a dichloromethane solution of the product. Red crystals of $[PPh_4][1,5\text{-}Rh_2Br_7(PEt_3)_2]$ (**3b**) suitable for X-ray analysis were obtained by slow evaporation of an acetone solution of the precipitate. $^{31}P\{^1H\}$ NMR (**3b**): δ 62.0 (d, 2P, J = 114 Hz), 30.7 (s, 1P).

Reaction between 3b and PR_3 (1 equiv; PR_3 = PMe_3 and PMe_2Ph). Formation of Edge-Sharing $[PPh_4][1,6,8\text{-}Rh_2Br_7(PEt_3)_2(PR_3)]$ Complexes. An acetone solution of 3b was prepared at room temperature, transferred to an NMR tube, and purged with argon. After the solution was cooled to –40 °C, 1 equiv of tertiary phosphine was introduced with a microsyringe. $^{31}P\{^1H\}$ NMR: $[PPh_4][1,6,8\text{-}Rh_2Br_7(PEt_3)_3]$, δ 54.9 (d, 1P, J = 114 Hz), 30.6 (s, 1P), (d, 2P, J = 81 Hz); $[PPh_4][1,6,8\text{-}Rh_2Br_7(PEt_3)_2(PMe_3)]$, δ 55.5 (d, 1P, J = 114 Hz), 30.6 (s, 1P), 1 (4d, 2P, $J_{P\text{-}P',trans}$ = 606, J = 82 Hz); $[PPh_4][1,6,8\text{-}Rh_2Br_7(PEt_3)_2(PMe_2Ph)]$, δ 55.7 (d, 1P, J = 115 Hz), 30.6 (s, 1P), 2 (4d, 2P, $J_{P\text{-}P',trans}$ = 598, J = 84 Hz).

Disproportionation of 3a. A dichloromethane solution of **3a** was prepared at –76 °C, transferred to an NMR tube, and purged with argon. The NMR tube was sealed under vacuum, kept at –20 °C, and tracked by $^{31}P\{^1H\}$ NMR spectroscopy for 1 day. The major products of disproportionation are $[NEt_4][1,5\text{-}Rh_2Br_7(PEt_3)_2]$, $1,2,6\text{-}Rh_2Br_6(PEt_3)_3$, and $[NEt_4][trans\text{-}RhBr_4(PEt_3)_2]$.

X-ray Crystallography

General Procedure. A suitable single crystal of each of the samples was chosen and glued to the tip of a glass fiber. X-ray diffraction experiments were carried out using one of two fully automated four-circle diffractometers: Enraf-Nonius CAD-4 and Syntex P3. The CAD-4 and P3 instruments were equipped with monochromated Mo Kα radiation (λ_0 = 0.7107 Å). Unit cell determination and data collection followed routine procedures previously described elsewhere in detail.[3] Oscillation photographs of the principal axes were taken to confirm the Laue class, symmetry, and the axial lengths and to evaluate crystal quality. In the case of data collection, three intense reflections which were previously chosen were monitored at regular intervals to check for variations in intensity. At the end of data collection azimuthal (ψ) scans were done on six reflections having an Eulerian angle χ = 90° ± 10 or 270° ± 10. The average of the ψ scans was the basis for the empirical absorption correction applied to the data set.[4] All data were also corrected for Lorentz and polarization effects. The structures were solved using the SHELXS 86 programs[5] and refined using the VAX-SDP software package[6] on a Local Area Vax Cluster. Relevant crystallographic data and information pertaining to the refinement results are listed in Table I.

$[PPh_4][1,5\text{-}Rh_2Cl_7(PEt_3)_2]$ (1). A red crystal was mounted on a quartz fiber with epoxy glue. Indexing gave a monoclinic cell, and Laue symmetry $2/m$ was confirmed by an oscillation photograph. The data had systematic absences indicating that the space group was $P2_1/c$ (No. 14). The structure was partially solved when Rh, Cl, and P atoms were found using the direct method (SHELXS 86). The rest of the non-hydrogen atoms were located by an alternating series of Fourier maps and least-squares refinement cycles. The model was refined to convergence with all Rh, Cl, P, and C atoms having anisotropic thermal parameters. Hydrogen atoms were not included in the refined model. Table II lists the final positional parameters.

$[PPh_4][1,6,8\text{-}Rh_2Cl_7(PEt_3)_2(PMe_3)]$ (2). Preliminary examination revealed that the crystal system was monoclinic, the lattice primitive, and the Laue group $2/m$. The data had systematic absences corresponding to the space group $P2_1/n$. The structure was partially solved when Rh, Cl, and P atoms were found using the direct method (SHELXS 86). The rest of the non-hydrogen atoms were located by an alternating series of Fourier maps and least-squares refinement cycles. The model was refined to convergence with all Rh, Cl, P, and C atoms having anisotropic thermal parameters. Hydrogen atoms were not included in the refined model. Table III lists the final positional parameters.

$[NEt_4][1,5\text{-}Rh_2Br_7(PEt_3)_2]$ (3a). A red-brown crystal was mounted on a quartz fiber with epoxy glue. Indexing gave a triclinic cell, and Laue symmetry $\bar{1}$ was confirmed by an oscillation photograph. The space group was chosen as $P\bar{1}$ (No. 2). The model was refined to convergence with all Rh, Br, and P atoms having anisotropic thermal parameters. Hydrogen atoms were not included in the refined model. Final atomic positional and isotropic displacement parameters are listed in Table IV.

$[PPh_4][trans\text{-}RhCl_4(PEt_3)_2]$ (4). A red-brown crystal was mounted on a quartz fiber with epoxy glue. Indexing gave a monoclinic cell, and Laue symmetry $2/m$ was confirmed by an oscillation photograph. The space group was determined as $P2_1/n$ (No. 14) based on the systematic absences. All of the non-hydrogen atoms in the molecule were refined with anisotropic thermal parameters. Final atomic positional and isotropic displacement parameters are listed in Table V.

Results

Structures. $[PPh_4][1,5\text{-}Rh_2Cl_7(PEt_3)_2]$ (1). An ORTEP drawing of the anion in compound 1 is shown in Figure 1. The positions of the two triethylphosphine ligands impart approximately C_2 symmetry to the anion. The geometry of the anion is that of a face-sharing bioctahedron, with three bridging chlorine atoms defining the triangular shared face. Each rhodium atom completes its coordination sphere with two terminal chlorine atoms and one triethylphosphine group in addition to three bridging chlorine ligands. Table VI lists bond distances and angles of the inner

(3) (a) Bino, A.; Cotton, F. A.; Fanwick, D. E. *Inorg. Chem.* **1979**, *18*, 3558. (b) Cotton, F. A.; Frenz, B. A.; Deganello, G.; Shaver, A. J. *J. Organomet. Chem.* **1973**, *50*, 227.
(4) North, A. C. T.; Phillips, D. C.; Mathews, F. S. *Acta Crystallogr., Sect. A: Cryst. Phys. Diffr., Theor. Gen. Crystallogr.* **1968**, *24*, 351.
(5) Sheldrick, G. M. SHELXS-86. Institut fur Anorganische Chemie der Universitat, Göttingen, FRG, 1986.
(6) SDP/V v3.0 Package of Programs. Frenz, B. A. and Associates, Inc., College Station, TX, 1985.

Table II. Positional and Isotropic Equivalent Thermal Parameters (Å) and Their Estimated Standard Deviations for $[PPh_4][1,5\text{-}Rh_2Cl_7(PEt_3)_2]$ (**1**)

atom	*x*	*y*	*z*	B_{iso},[a] Å^2
Rh(1)	0.78481(4)	0.18814(7)	0.02088(3)	2.68(1)
Rh(2)	0.85467(4)	0.20533(7)	0.13158(3)	2.69(2)
Cl(1)	0.7753(2)	0.0137(2)	0.0843(1)	3.47(5)
Cl(2)	0.9155(1)	0.2080(3)	0.0533(1)	3.11(5)
Cl(3)	0.7586(1)	0.3519(3)	0.0934(1)	3.45(5)
Cl(4)	0.6531(1)	0.1691(3)	−0.0013(1)	4.30(6)
Cl(5)	0.8015(2)	0.3780(3)	−0.0323(1)	4.47(6)
Cl(6)	0.7810(2)	0.1984(3)	0.2034(1)	4.17(6)
Cl(7)	0.9419(2)	0.0408(3)	0.1643(1)	4.11(6)
P(1)	0.8097(2)	0.0374(3)	−0.0405(1)	3.10(5)
P(2)	0.9320(2)	0.3801(3)	0.1603(1)	3.49(6)
P(3)	0.4488(2)	0.3024(2)	0.36136(9)	2.67(5)
C(1)	0.7644(8)	0.409(1)	0.3992(4)	6.0(3)
C(2)	0.792(1)	0.480(2)	0.3537(5)	9.3(5)
C(3)	0.9143(6)	0.490(1)	0.4474(5)	4.5(3)
C(4)	0.9591(9)	0.352(1)	0.4308(6)	6.1(4)
C(5)	0.7700(9)	0.637(1)	0.4743(5)	7.1(3)
C(6)	0.202(2)	0.255(2)	0.067(1)	16 (1)
C(7)	0.9324(7)	0.408(1)	0.2277(4)	4.7(3)
C(8)	0.0303(8)	0.784(1)	0.2418(5)	6.3(3)
C(9)	0.9008(8)	0.555(1)	0.1377(5)	4.9(3)
C(10)	0.918(1)	0.582(2)	0.0798(6)	7.8(5)
C(11)	0.0348(7)	0.347(1)	0.1429(5)	5.2(3)
C(12)	0.0939(7)	0.468(1)	0.1624(6)	8.1(4)
C(13)	0.4739(6)	0.489(1)	0.3571(4)	3.2(2)
C(14)	0.4201(6)	0.589(1)	0.3767(4)	3.1(2)
C(15)	0.4389(6)	0.732(1)	0.3704(4)	3.4(2)
C(16)	0.4940(7)	0.273(1)	0.1505(4)	4.4(2)
C(17)	0.5621(7)	0.672(1)	0.3302(5)	5.6(3)
C(18)	0.5437(6)	0.527(4)	0.3363(4)	4.1(2)
C(19)	0.3674(5)	0.256(1)	0.3199(3)	2.6(2)
C(20)	0.3091(6)	0.357(1)	0.3099(4)	3.3(2)
C(21)	0.2428(7)	0.316(1)	0.2795(4)	4.0(2)
C(22)	0.7636(7)	0.681(1)	0.2371(4)	3.8(2)
C(23)	0.7068(6)	0.579(1)	0.2254(5)	5.0(3)
C(24)	0.6419(6)	0.620(1)	0.1948(4)	4.4(2)
C(25)	0.4266(6)	0.252(1)	0.4234(4)	3.3(2)
C(26)	0.4606(6)	0.328(1)	0.4638(4)	3.9(2)
C(27)	0.5494(7)	0.727(1)	0.4886(4)	4.1(2)
C(28)	0.4086(7)	0.343(1)	0.02025(4)	3.6(2)
C(29)	0.6253(8)	0.508(1)	0.0211(5)	5.0(3)
C(30)	0.6175(7)	0.635(1)	0.0677(5)	4.3(3)
C(31)	0.4683(6)	0.706(1)	0.1573(4)	3.0(2)
C(32)	0.4119(6)	0.656(1)	0.1220(4)	3.2(2)
C(33)	0.3448(6)	0.594(1)	0.1381(4)	4.1(2)
C(34)	0.3278(7)	0.575(1)	0.1891(5)	6.4(3)
C(35)	0.3858(8)	0.630(1)	0.2257(5)	5.9(3)
C(36)	0.4503(7)	0.689(1)	0.2093(4)	4.2(3)

[a] Values for anisotropically refined atoms are given in the form of the equivalent isotropic displacement parameter defined as $(4/3)[a^2\beta_{11} + b^2\beta_{22} + c^2\beta_{33} + ab(\cos\gamma)\beta_{12} + ac(\cos\beta)\beta_{13} + bc(\cos\alpha)\beta_{23}$.

Table III. Positional and Isotropic Equivalent Thermal Parameters (Å^2) and Their Estimated Standard Deviations for $[PPh_4][1,6,8\text{-}Rh_2Cl_7(PEt_3)_2(PMe_3)]$ (**2**)[a]

atom	*x*	*y*	*z*	B_{iso},[a] Å^2
Rh(1)	0.25915(6)	0.24264(4)	−0.04570(2)	2.79(1)
Rh(2)	0.24901(6)	0.21460(4)	0.09580(3)	3.29(1)
Cl(1)	0.3046(2)	0.3163(1)	0.04018(8)	3.23(4)
Cl(2)	0.2098(2)	0.1451(1)	0.01641(9)	3.80(5)
Cl(3)	0.3104(2)	0.3457(1)	−0.09789(8)	3.78(5)
Cl(4)	0.4616(2)	0.2006(1)	−0.04285(8)	3.85(5)
Cl(5)	0.0564(2)	0.2854(1)	−0.04953(9)	4.12(5)
Cl(6)	0.1859(2)	0.1099(2)	0.1463(1)	5.90(6)
Cl(7)	0.2905(3)	0.2935(2)	0.16898(9)	5.75(6)
P(1)	0.2120(2)	0.1727(1)	−0.1179(1)	4.08(5)
P(2)	0.4515(2)	0.1655(1)	0.10624(9)	3.54(5)
P(3)	0.0459(2)	0.2580(2)	0.0975(1)	4.78(6)
P(4)	−0.2675(2)	0.3944(1)	−0.13810(8)	3.08(4)
C(1)	0.603(1)	0.4095(7)	0.3994(5)	9.3(4)
C(2)	0.330(2)	0.521(1)	0.587(8)	13.9(7)
C(3)	0.3411(9)	0.1338(6)	0.8473(4)	6.0(2)
C(4)	0.418(1)	0.1912(8)	0.8222(4)	7.2(3)
C(5)	0.6181(9)	0.2750(6)	0.3327(4)	5.5(2)
C(6)	0.601(1)	0.3175(8)	0.2780(4)	7.2(3)
C(7)	0.4891(9)	0.1412(6)	0.1757(3)	5.2(2)
C(8)	0.622(1)	0.1110(8)	0.1872(5)	7.(3)
C(9)	0.4884(8)	0.0783(5)	0.0685(4)	4.5(2)
C(10)	0.411(1)	0.0052(6)	0.0829(5)	6.2(3)
C(11)	0.5768(8)	0.2295(5)	0.0872(4)	4.3(2)
C(12)	0.594(1)	0.3026(6)	0.1219(4)	5.6(2)
C(13)	0.492(1)	0.2422(7)	0.6647(4)	7.9(3)
C(14)	0.4301(9)	0.2977(7)	0.5591(5)	6.5(3)
C(15)	0.5168(9)	0.1411(6)	0.5779(4)	5.4(2)
C(16)	0.2217(7)	0.0779(5)	0.4290(3)	3.1(2)
C(17)	0.3093(8)	0.0303(5)	0.4547(3)	4.0(2)
C(18)	0.7093(9)	−0.0052(5)	0.4939(3)	4.4(2)
C(19)	0.6874(9)	0.4706(5)	0.0307(4)	4.4(2)
C(20)	0.6016(8)	0.4213(5)	0.0061(3)	4.2(2)
C(21)	0.6180(8)	0.3978(5)	0.9538(3)	3.9(2)
C(22)	0.3572(7)	0.0555(5)	0.3335(3)	3.2(2)
C(23)	0.6665(8)	0.0007(6)	0.7041(4)	5.0(2)
C(24)	0.5707(9)	0.0418(7)	0.7241(4)	6.4(3)
C(25)	0.4497(9)	0.0245(6)	0.7060(4)	5.6(2)
C(26)	0.5718(8)	0.0343(6)	0.3301(4)	4.7(2)
C(27)	0.4774(7)	0.0758(5)	0.3508(3)	3.8(2)
C(28)	0.5934(7)	0.4228(5)	0.8268(3)	3.2(2)
C(29)	0.544(1)	0.3809(6)	0.7858(4)	6.5(3)
C(30)	0.437(1)	0.4057(7)	0.7579(5)	9.3(3)
C(31)	0.3816(9)	0.4750(6)	0.7695(4)	5.5(3)
C(32)	0.4300(9)	0.5161(6)	0.8131(4)	5.3(2)
C(33)	0.464(1)	0.5100(6)	0.1584(4)	5.2(2)
C(34)	0.7536(7)	0.2907(4)	0.8568(3)	3.2(2)
C(35)	0.2764(7)	0.2401(5)	0.3083(3)	3.6(2)
C(36)	0.2873(8)	0.3208(5)	0.3036(4)	4.4(2)
C(37)	0.2783(8)	0.3686(5)	0.3482(4)	4.6(2)
C(38)	0.7575(9)	0.1643(5)	0.8965(4)	5.2(2)
C(39)	0.2440(8)	0.2539(5)	0.4019(4)	4.0(2)

[a] Values for anisotropically refined atoms are given in the form of the equivalent isotropic displacement parameter defined as $(4/3)[a^2\beta_{11} + b^2\beta_{22} + c^2\beta_{33} + ab(\cos\gamma)\beta_{12} + ac(\cos\beta)\beta_{13} + bc(\cos\alpha)\beta_{23}$.

portion of the anion. All of the bridging Rh–Cl bonds are longer than the terminal Rh–Cl bonds, as is normal. The Rh–Cl bonds which are trans to Rh–P bonds (2.557[3] Å) are longer than those trans to Rh–Cl bonds (2.366[3] Å) due to the trans influence by the phosphine ligands. Deviations of angles from those expected for the ideal geometry signal the absence of a metal–metal bond. The average $Rh\text{–}Cl_{br}\text{–}Rh$ angle is 81.57[8]°, and that of $Cl_{br}\text{–}Rh\text{–}Cl_{br}$ is 81.94[9]°. The Rh–Rh interatomic distance is 3.18[1] Å.

$[PPh_4][1,6,8\text{-}Rh_2Cl_7(PEt_3)_2(PMe_3)]$ (2). The structure of the anion is shown in Figure 2, and Table VII gives bond distances and angles for the inner part. As will be pointed out later, the NMR spectrum cannot distinguish between the 1,6,8- and the 2,6,8- or the 4,6,8-isomers. The crystal structure shows that the first one is correct. This structure displays all of the expected consequences of (a) there being no Rh–Rh bond, and (b) the phosphine in position 1 having a marked trans influence.

$[NEt_4][1,5\text{-}Rh_2Br_7(PEt_3)_2]$ (3a). An ORTEP drawing of the anion in compound **3a** is shown in Figure 3. The face-sharing rhodium dinuclear anion has no crystallographically imposed symmetry, but the inner set of atoms in the anion possesses C_2 symmetry. Table VIII lists bond distances and angles of the inner portion of the molecule. As expected, all of the $Rh\text{–}Br_t$ bond distances are shorter than the bridging ones, but the latter are divided into two very distinct groups. The bridging bromine atoms that are trans to phosphine ligands have longer Rh–Br bond distances (average 2.647[2] Å) than those trans to bromine atoms (average 2.494[3] Å), in accord with the trans influence of phosphine ligands. There is no metal–metal bond interaction, the Rh–Rh interatomic distance being about 3.327 Å. Deviations of angles from those expected for the ideal geometry are consistent with the absence of metal–metal bond interaction. The average $Rh\text{–}Br_{br}\text{–}Rh$ is 81.65[9]° and that of $Br_{br}\text{–}Rh\text{–}Br_{br}$ is 81.97[9]°.

$[PPh_4][trans\text{-}RhCl_4(PEt_3)_2]$ (4). The geometry of the anion $[trans\text{-}RhCl_4(PEt_3)_2]$ in its crystalline tetraphenylphosphonium salt is shown in Figure 4. Table IX lists relevant bond lengths

Table IV. Positional and Isotropic Equivalent Thermal Parameters (Å²) and Their Estimated Standard Deviations for $[NEt_4][1,5\text{-}Rh_2Br_7(PEt_3)_2]$ (**3a**)

atom	x	y	z	B_{iso},[a] Å²
Rh(1)	0.48451(9)	0.76810(9)	0.4895(1)	3.87(4)
Rh(2)	0.50517(9)	0.78768(9)	0.7609(1)	4.18(4)
Br(1)	0.3766(1)	0.8253(1)	0.6042(2)	5.55(6)
Br(2)	0.5634(1)	0.8392(1)	0.6163(2)	4.34(5)
Br(3)	0.5401(1)	0.6641(1)	0.6559(2)	5.27(6)
Br(4)	0.6027(1)	0.7079(1)	0.3979(2)	4.97(5)
Br(5)	0.4075(1)	0.6879(1)	0.3883(2)	6.10(6)
Br(6)	0.4342(1)	0.7351(2)	0.8837(2)	6.81(7)
Br(7)	0.4626(1)	0.9167(1)	0.8413(2)	6.02(6)
P(1)	0.4339(3)	0.8632(3)	0.3569(4)	4.6(1)
P(2)	0.6199(3)	0.7533(3)	0.8845(4)	5.0(2)
C(1)	0.442(1)	0.827(1)	0.216(2)	5.1(5)*
C(2)	0.406(1)	0.895(1)	0.130(2)	6.4(5)*
C(3)	0.326(1)	0.921(1)	0.354(2)	6.7(6)*
C(4)	0.265(1)	0.878(1)	0.322(2)	8.9(7)*
C(5)	0.485(1)	0.941(1)	0.374(2)	5.3(5)*
C(6)	0.575(1)	0.917(1)	0.357(2)	7.4(6)*
C(7)	0.32091)	0.354(1)	0.110(2)	7.9(7)*
C(8)	0.638(2)	0.598(2)	0.924(3)	11.9(9)*
C(9)	0.302(1)	0.207(1)	0.146(2)	5.5(5)*
C(10)	0.316(1)	0.119(1)	0.136(2)	6.5(5)*
C(11)	0.398(1)	0.218(1)	-0.024(2)	6.3(5)*
C(12)	0.679(1)	0.754(1)	0.113(2)	7.6(6)*
N(1)	0.6410(6)	0.4617(6)	0.3153(8)	0.9(2)*
C(25)	0.674(2)	0.369(2)	0.330(3)	13(1)*
C(26)	0.752(2)	0.317(2)	0.384(2)	9.5(8)*
C(27)	0.598(2)	0.493(2)	0.428(3)	16(1)*
C(28)	0.335(2)	0.512(2)	0.466(2)	9.8(8)*
C(29)	0.703(3)	0.497(3)	0.297(4)	18(2)*
C(30)	0.735(2)	0.498(3)	0.196(4)	18(2)*
C(31)	0.552(2)	0.485(2)	0.223(3)	17(1)*
3(32)	0.519(2)	0.553(2)	0.177(3)	21(1)*

[a] Starred values denote atoms that were rfined isotropically. Values for anisotropically refined atoms are given in the form of the equivalent isotropic displacement parameter defined as $(4/3)[a^2\beta_{11} + b^2\beta_{22} + c^2\beta_{33} + ab(\cos\gamma)\beta_{12} + ac(\cos\beta)\beta_{13} + bc(\cos\alpha)\beta_{23}$.

and angles. The rhodium atom displays distorted octahedral coordination, with a square-planar $RhCl_4$ unit and axial coordination of the triethylphosphine molecules. The idealized local symmetry of the rhodium atom in $RhCl_4P_2$ coordination is D_{4h}, with the C_4 axis passing through the P(1)–Rh–P(2) bond vectors. The average Rh–Cl distance, 2.358[2] Å, is similar to that observed for the rhodium(III) complex *mer*-$RhCl_3(PMe_2Ph)_3$.[7] The average Rh–P distance, 2.356[2] Å, is also close to those in other rhodium(III) compounds.

NMR Results. The crystallographic results show that the 1,5-$Rh_2Cl_7(PEt_3)_2$ anion has C_2 symmetry, and it would be expected to give one doublet in the $^{31}P\{^1H\}$ NMR spectrum. That doublet is observed at 60.0 ppm and J_{Rh-P} is 116 Hz. The possibility of 1,5/1,4 isomerization for this face-sharing rhodium dinuclear compound was examined at or below room temperature. No additional signal attributable to the other isomer was detected in this temperature range.

The $^{31}P\{^1H\}$ data for the $[1,5\text{-}Rh_2Br_7(PEt_3)_2]^-$ ion are quite similar and here again, at and below room temperature no indication of isomerization to the 1,4-isomer was observed.

A FSBO/ESBO interconversion has been studied for these 1,5-isomers. The addition of 1 equiv of triethylphosphine to $[PPh_4][1,5\text{-}Rh_2Cl_7(PEt_3)_2]$ in acetone at −30 °C led to an edge-sharing rhodium dinuclear compound. The $^{31}P\{^1H\}$ NMR spectrum, Figure 5, shows two doublets in a 1:2 ratio. The downfield doublet at 56.6 ppm (J = 115 Hz) is due to the Rh–P coupling trans to chloride while the other at 15.3 ppm (J = 81 Hz) corresponds to phosphines trans to each other. The singlet at δ 29.9 arises from PPh_4.

(7) Skapski, A. C.; Stephens, F. A. *J. Chem. Soc., Dalton Trans.* **1973**, 1789.

Table V. Positional and Isotropic Equivalent Thermal Parameters (Å²) and Their Estimated Standard Deviations for $[PPh_4][trans\text{-}RhCl_4(PEt_3)_2]$ (**4**)

atom	x	y	z	B_{iso} (Å²)
Rh(1)	0.11052(3)	0.62791(2)	0.79736(2)	3.261(9)
Cl(1)	0.2638(1)	0.61516(8)	0.74026(8)	4.22(3)
Cl(2)	0.2075(1)	0.71980(8)	0.87889(8)	4.86(4)
Cl(3)	-0.0428(1)	0.63796(9)	0.85467(9)	5.35(4)
Cl(4)	0.0096(1)	0.53920(9)	0.71422(9)	5.85(4)
P(1)	0.0301(1)	0.7178(1)	0.70681(9)	4.54(4)
P(2)	0.1860(1)	0.53543(9)	0.88543(9)	4.65(3)
P(3)	0.3036(1)	0.59621(8)	0.42866(7)	2.94(3)
C(1)	0.4179(7)	0.3128(4)	0.7779(5)	6.8(2)
C(2)	0.2941(7)	0.3197(5)	0.7818(5)	8.4(2)
C(3)	0.6276(6)	0.2255(6)	0.8094(5)	8.5(2)
C(4)	0.666(1)	0.2829(8)	0.7639(6)	12.4(4)
C(5)	0.4550(7)	0.1927(5)	0.8860(4)	6.7(2)
C(6)	0.4972(9)	0.2554(6)	0.9493(5)	9.3(3)
C(7)	0.344(6)	0.5082(4)	0.8919(4)	5.6(2)
C(8)	0.5809(6)	0.4305(5)	0.0760(4)	6.6(2)
C(9)	0.3187(7)	0.0620(5)	0.5188(4)	8.0(2)
C(10)	0.231(1)	0.5006(7)	0.0408(5)	13.5(3)
C(11)	0.6166(6)	0.571(4)	0.3684(5)	7.8(2)
C(12)	0.4935(8)	0.599(6)	0.3755(7)	10.5(3)
C(13)	0.1930(4)	0.6613(3)	0.3895(3)	3.5(1)
C(14)	0.7874(6)	0.2606(4)	0.6017(4)	5.9(2)
C(15)	0.3755(7)	0.2872(4)	0.1326(5)	7.0(2)
C(16)	0.4794(5)	0.2609(4)	0.1728(4)	5.3(2)
C(17)	0.4922(5)	0.1860(4)	0.1800(4)	6.2(2)
C(18)	0.4075(6)	0.1355(4)	0.1488(4)	5.9(2)
C(19)	0.3627(4)	0.5535(3)	0.3579(3)	3.2(1)
C(20)	0.5209(5)	0.4468(3)	0.6359(3)	4.0(1)
C(21)	0.4806(5)	0.4839(4)	0.6918(4)	5.0(1)
C(22)	0.4481(6)	0.4792(4)	0.2519(3)	5.2(2)
C(23)	0.3327(6)	0.4790(4)	0.2470(3)	5.3(2)
C(24)	0.2110(5)	0.0172(4)	0.2004(3)	4.5(1)
C(25)	0.2457(4)	0.5228(3)	0.4743(3)	3.2(1)
C(26)	0.2807(5)	0.4488(3)	0.4695(3)	3.9(1)
C(27)	0.7419(5)	0.1074(3)	0.0109(4)	4.7(1)
C(28)	0.6718(5)	0.0883(4)	0.0568(3)	5.3(2)
C(29)	0.6376(5)	0.0155(4)	0.0618(4)	5.7(2)
C(30)	0.8273(5)	0.4591(4)	0.4809(3)	4.8(1)
C(31)	0.4091(4)	0.6463(3)	0.4955(3)	3.3(1)
C(32)	0.5863(6)	0.3637(4)	0.4291(3)	5.1(2)
C(33)	0.5141(7)	0.3195(4)	0.3768(4)	6.6(2)
C(34)	0.4456(6)	0.2673(4)	0.4016(4)	6.1(2)
C(35)	0.4507(5)	0.2579(4)	0.4756(4)	5.1(2)
C(36)	0.5230(5)	0.3005(3)	0.5281(3)	4.1(1)

[a] Values for anisotropically refined atoms are given in the form of the equivalent isotropic displacement parameter defined as $(4/3)[a^2\beta_{11} + b^2\beta_{22} + c^2\beta_{33} + ab(\cos\gamma)\beta_{12} + ac(\cos\beta)\beta_{13} + bc(\cos\alpha)\beta_{23}$.

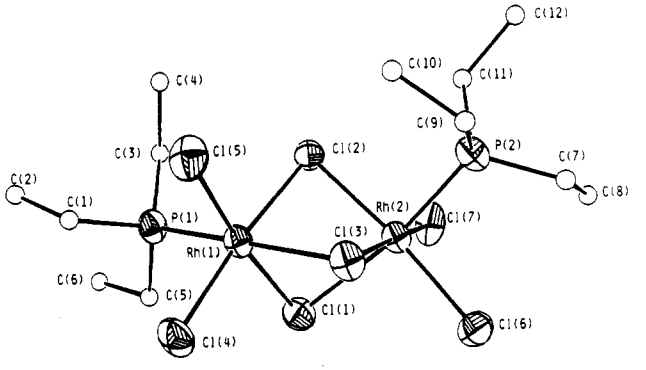

Figure 1. ORTEP drawing for $[PPh_4][1,5\text{-}Rh_2Cl_7(PEt_3)_2]$ (**1**).

The $^{31}P\{^1H\}$ NMR spectrum shows that the addition of 1 equiv of triethylphosphine to $[PPh_4][1,5\text{-}Rh_2Cl_7(PEt_3)_2]$ affords stereospecifically only one edge-sharing $Rh_2(\mu\text{-}Cl)_2Cl_5(PEt_3)_3$ anionic isomer. Additional experiments were done to support and extend this observation, namely the addition of trimethylphosphine or dimethylphenylphosphine to $[PPh_4][1,5\text{-}Rh_2Cl_7(PEt_3)_2]$. The addition of 1 equiv of trimethylphosphine to $[PPh_4][1,5\text{-}Rh_2Cl_7(PEt_3)_2]$ at −30 °C produces an ESBO isomer that gives

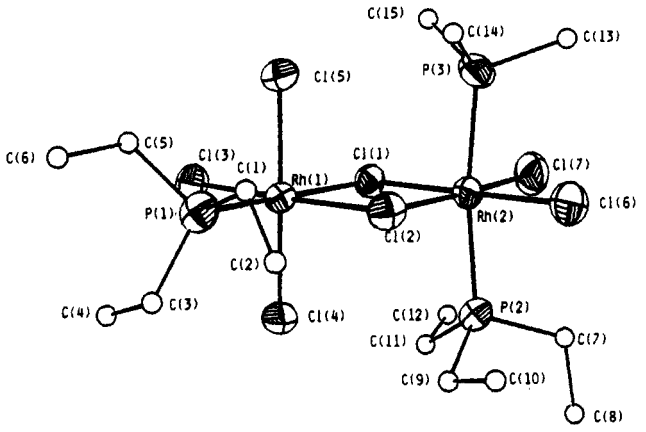

Figure 2. ORTEP drawing for $[PPh_4][1,6,8\text{-}Rh_2Cl_7(PEt_3)_2(PMe_3)]$ (**2**).

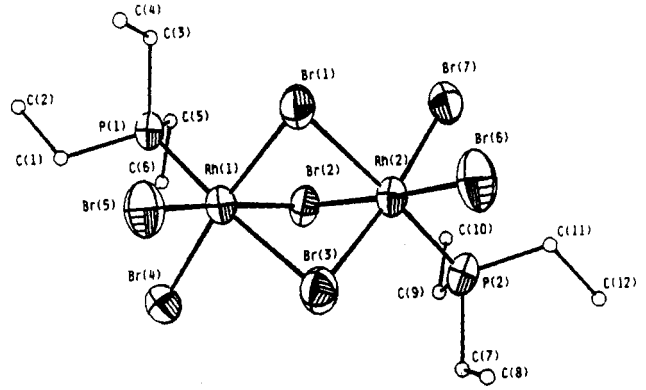

Figure 3. ORTEP drawing for $[NEt_4][1,5\text{-}Rh_2Br_7(PEt_3)_2]$ (**3a**).

Table VI. Selected Bond Distances (Å) and Angles (deg) for $[PPh_4][1,5\text{-}Rh_2Cl_7(PEt_3)_2]$ (**1**)

Bond Distances			
Rh(1)–Cl(1)	2.379(3)	Rh(2)–Cl(1)	2.576(3)
Rh(1)–Cl(2)	2.369(2)	Rh(2)–Cl(2)	2.362(3)
Rh(1)–Cl(3)	2.537(3)	Rh(2)–Cl(3)	2.355(3)
Rh(1)–Cl(4)	2.305(3)	Rh(2)–Cl(6)	2.322(3)
Rh(1)–Cl(5)	2.317(3)	Rh(2)–Cl(7)	2.308(3)
Rh(1)–P(1)	2.228(3)	Rh(2)–P(2)	2.236(3)
Bond Angles			
Cl(1)–Rh(1)–Cl(2)	82.65(9)	Cl(1)–Rh(2)–Cl(2)	78.69(8)
Cl(1)–Rh(1)–Cl(3)	81.96(8)	Cl(1)–Rh(2)–Cl(3)	81.56(8)
Cl(1)–Rh(1)–Cl(4)	92.8(1)	Cl(1)–Rh(2)–Cl(6)	95.95(9)
Cl(1)–Rh(1)–Cl(5)	172.1(1)	Cl(1)–Rh(2)–Cl(7)	91.99(9)
Cl(1)–R(1)–P(1)	95.78(9)	Cl(1)–Rh(2)–P(2)	170.4(1)
Cl(2)–Rh(1)–Cl(3)	81.34(8)	Cl(2)–Rh(2)–Cl(3)	85.41(9)
Cl(2)–Rh(1)–C(4)	173.4(1)	Cl(2)–Rh(2)–Cl(6)	173.3(1)
Cl(2)–Rh(1)–Cl(5)	92.1(1)	Cl(2)–Rh(2)–Cl(7)	93.21(9)
Cl(2)–Rh(1)–P(1)	97.49(9)	Cl(2)–Rh(2)–P(2)	91.9(1)
Cl(3)–Rh(1)–Cl(4)	93.40(9)	Cl(3)–Rh(2)–Cl(6)	89.8(1)
Cl(3)–Rh(1)–Cl(5)	91.41(9)	Cl(3)–Rh(2)–Cl(7)	173.56(9)
Cl(3)–Rh(1)–P(1)	177.56(9)	Cl(3)–Rh(2)–P(2)	96.15(9)
Cl(4)–Rh(1)–Cl(5)	91.9(1)	Cl(6)–Rh(2)–Cl(7)	91.0(1)
Cl(4)–Rh(1)–P(1)	87.6(1)	Cl(6)–Rh(2)–P(2)	93.3(1)
Cl(5)–Rh(1)–P(1)	90.8(1)	Cl(7)–Rh(2)–P(2)	90.2(1)
Rh(1)–Cl(1)–R(2)	79.59(7)	Rh(1)–Cl(2)–Rh(2)	84.28(8)
Rh(1)–Cl(3)–Rh(1)	80.84(8)		

one doublet at 56.3 ppm and four doublets centered at 10 ppm in a 1:2 ratio, as shown in Figure 6. The downfield doublet at 56.3 ppm (J = 116 Hz) arises from phosphine trans to chloride whereas the quartet of doublets centered at 10 ppm ($J_{P-P,trans}$ = 636 Hz, J_{Rh-P} = 82 Hz) comes from a trans pair of phosphines. Therefore, the $^{31}P\{^1H\}$ NMR spectrum of the reaction product of 1 equiv of trimethylphosphine with $[PPh_4][1,5\text{-}Rh_2Cl_7(PEt_3)_2]$ shows that there are three distinct phosphines, one trans to chloride and the other two trans to each other, and that the trimethylphosphine is located at an axial site on the edge-sharing

Table VII. Selected Bond Distances (Å) and Angles (deg) for $[PPh_4][1,6,8\text{-}Rh_2Cl_7(PEt_3)_2(PMe_3)]$ (**2**)

Bond Distances			
Rh(1)–Cl(1)	2.551(2)	Rh(2)–Cl(1)	2.356(2)
Rh(1)–Cl(2)	2.391(2)	Rh(2)–Cl(2)	2.366(2)
Rh(1)–Cl(3)	2.307(2)	Rh(2)–Cl(6)	2.344(3)
Rh(1)–Cl(4)	2.333(2)	Rh(2)–Cl(7)	2.330(3)
Rh(1)–Cl(5)	2.340(2)	Rh(2)–P(2)	2.377(2)
Rh(1)–P(1)	2.233(1)	Rh(2)–P(3)	2.354(3)
Bond Angles			
Cl(1)–Rh(1)–Cl(2)	79.92(7)	Cl(1)–Rh(2)–Cl(2)	84.55(7)
Cl(1)–Rh(1)–Cl(3)	93.85(7)	Cl(1)–Rh(2)–Cl(6)	176.17(8)
Cl(1)–Rh(1)–Cl(4)	89.40(7)	Cl(1)–Rh(2)–Cl(7)	89.96(8)
Cl(1)–Rh(1)–Cl(5)	90.97(7)	Cl(1)–Rh(2)–P(2)	93.42(8)
Cl(1)–Rh(1)–P(1)	176.22(8)	Cl(1)–Rh(2)–P(3)	93.01(8)
Cl(2)–Rh(1)–Cl(3)	173.76(8)	Cl(2)–Rh(2)–Cl(6)	91.91(8)
Cl(2)–Rh(1)–Cl(4)	90.17(8(	Cl(2)–Rh(2)–Cl(7)	174.46(9)
Cl(2)–Rh(1)–Cl(5)	89.90(8)	Cl(2)–Rh(2)–P(2)	92.17(8)
Cl(2)–Rh(1)–P(1)	96.50(8)	Cl(2)–Rh(2)–P(3)	92.92(8)
Cl(3)–Rh(1)–Cl(4)	89.66(4)	Cl(6)–Rh(2)–Cl(7)	93.55(9)
Cl(3)–Rh(1)–Cl(5)	89.76(8)	Cl(6)–Rh(2)–P(2)	88.17(9)
Cl(3)–Rh(1)–P(1)	89.72(8)	Cl(6)–Rh(2)–P(3)	85.69(9)
Cl(4)–Rh(1)–Cl(5)	179.34(8)	Cl(7)–Rh(2)–P(2)	88.89(9)
Cl(4)–Rh(1)–P(1)	91.86(9)	Cl(7)–Rh(2)–Rh(3)	86.6(1)
Cl(5)–Rh(1)–P(1)	87.80(9)	P(2)–Rh(2)–P(3)	172.15(9)
Rh(1)–Cl(1)–Rh(2)	95.67(7)	Rh(1)–Cl(2)–Rh(2)	99.84(8)

Table VIII. Selected Bond Distances (Å) and Angles (deg) for $[NEt_4][1,5\text{-}Rh_2Br_7(PEt_3)_2]$ (**3a**)

Bond Distances			
Rh(1)–Br(1)	2.486(3)	Rh(2)–Br(1)	2.644(2)
Rh(1)–Br(2)	2.496(3)	Rh(2)–Br(2)	2.490(3)
Rh(1)–Br(3)	2.654(2)	Rh(2)–Br(3)	2.504(3)
Rh(1)–Br(4)	2.450(3)	Rh(2)–Br(6)	2.447(3)
Rh(1)–Br(5)	2.440(3)	Rh(2)–Br(7)	2.446(3)
Rh(1)–P(1)	2.257(5)	Rh(2)–P(2)	2.244(5)
Bond Angles			
Br(1)–Rh(1)–Br(2)	83.22(9)	Br(1)–Rh(2)–Br(2)	80.18(8)
Br(1)–Rh(1)–Br(3)	82.28(8)	Br(1)–Rh(2)–Br(3)	82.13(8)
Br(1)–Rh(1)–Br(4)	172.9(1)	Br(1)–Rh(2)–Br(6)	82.76(9)
Br(1)–Rh(1)–Br(5)	93.2(1)	Br(1)–Rh(2)–Br(7)	91.66(8)
Br(1)–Rh(1)–P(1)	94.3(1)	Br(1)–Rh(2)–P(2)	175.9(2)
Br(2)–Rh(1)–Br(3)	80.40(8)	Br(2)–Rh(2)–Br(3)	83.52(9)
Br(2)–Rh(1)–Br(4)	91.67(9)	Br(2)–Rh(2)–Br(6)	172.5(1)
Br(2)–Rh(1)–Br(5)	172.0(1)	Br(2)–Rh(2)–Br(7)	91.85(9)
Br(2)–Rh(1)–P(1)	97.0(2)	Br(2)–Rh(2)–P(2)	96.5(2)
Br(3)–Rh(1)–Br(4)	92.04(8)	Br(3)–Rh(2)–Br(6)	93.2(1)
Br(3)–Rh(1)–Br(5)	92.06(9)	Br(3)–Rh(2)–Br(7)	172.79(9)
Br(3)–Rh(1)–P(1)	175.9(2)	Br(3)–Rh(2)–P(2)	95.2(2)
Br(4)–Rh(1)–Br(5)	91.26(9)	Br(6)–Rh(2)–Br(7)	90.8(1)
Br(4)–Rh(1)–P(1)	91.2(2)	Br(6)–Rh(2)–P(2)	90.5(2)
Br(5)–Rh(1)–P(1)	90.4(2)	Br(7)–Rh(2)–P(2)	90.8(2)
Rh(1)–Br(1)–Rh(2)	80.77(7)	Rh(1)–Br(2)–Rh(2)	83.70(9)
Rh(1)–Br(3)–Rh(2)	80.27(7)		

$[PPh_4][1,6,8\text{-}Rh_2Cl_7(PEt_3)_2(PMe_3)]$ product. The addition of dimethylphenylphosphine to $[PPh_4][1,5\text{-}Rh_2Cl_7(PEt_3)_2]$ at −30 °C again affords only one edge-sharing isomer. For numerical data see the Experimental Section. The Rh–P coupling of the downfield doublet at 56.6 ppm arises from triethylphosphine trans to chloride. For the quartet of doublets, $J_{P-P,trans}$ is 624 Hz, and J_{Rh-P} is 85 Hz.

The addition of 2 equiv of triethylphosphine to $[PPh_4][1,6,8\text{-}Rh_2Cl_7(PEt_3)_3]$ in acetone at room temperature produced the spectrum shown in Figure 7. This spectrum is due to two mononuclear rhodium(III) compounds, viz., *mer*-$RhCl_3(PEt_3)_3$ and $[PPh_4][trans\text{-}RhCl_4(PEt_3)_2]$. In the *mer*-$RhCl_3(PEt_3)_3$ compound, the two triplets centered at 26.8 ppm arise from phosphine trans to chloride (J_{Rh-P} = 112 Hz and $J_{P-P,cis}$ = 24 Hz) and the two doublets from the two phosphines trans to each other (J_{Rh-P} = 84 Hz and $J_{P-P,cis}$ = 25 Hz). The doublet centered at 12.9 ppm and the singlet at 30.0 ppm come from $[PPh_4][trans$-

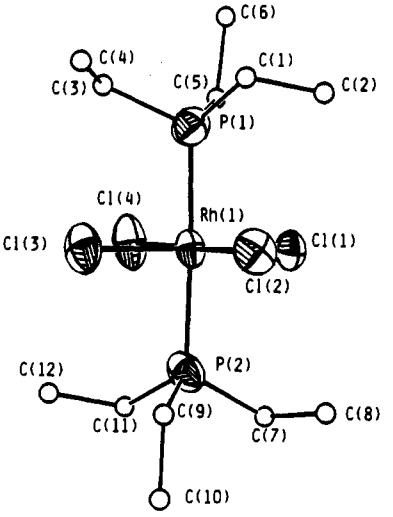

Figure 4. ORTEP drawing for $[PPh_4][trans\text{-}RhCl_4(PEt_3)_2]$ (**4**).

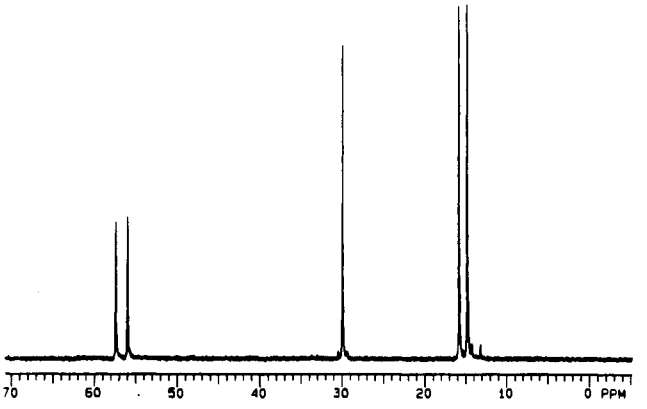

Figure 5. $^{31}P\{^1H\}$ NMR spectrum of **1** + PEt_3.

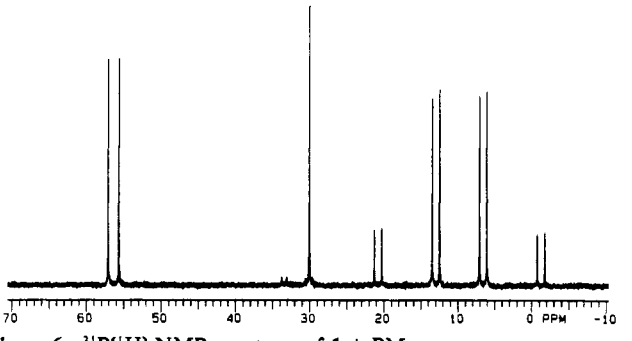

Figure 6. $^{31}P\{^1H\}$ NMR spectrum of **1** + PMe_3.

Table IX. Selected Bond Distances (Å) and Angles (deg) for $[PPh_4][trans\text{-}RhCl_4(PEt_3)_2]$ (**4**)

Bond Distances			
Rh(1)–Cl(1)	2.366(2)	Rh(1)–Cl(3)	2.365(2)
Rh(1)–Cl(2)	2.352(2)	Rh(1)–Cl(4)	2.347(2)
Rh(1)–P(1)	2.361(2)	Rh(1)–P(2)	2.350(2)
Bond Angles			
Cl(1)–Rh(1)–Cl(2)	91.11(6)	Cl(1)–Rh(1)–Cl(3)	178.84(6)
Cl(1)–Rh(1)–Cl(4)	89.63(6)	Cl(1)–Rh(1)–P(1)	89.48(6)
Cl(1)–Rh(1)–P(2)	91.02(6)	Cl(2)–Rh(1)–Cl(3)	89.66(6)
Cl(2)–Rh(1)–Cl(4)	178.15(6)	Cl(2)–Rh(1)–P(1)	92.79(5)
Cl(2)–Rh(1)–P(2)	89.08(5)	Cl(3)–Rh(1)–Cl(4)	89.63(6)
Cl(3)–Rh(1)–P(1)	91.36(6)	Cl(3)–Rh(1)–P(2)	88.12(6)
Cl(4)–Rh(1)–P(1)	85.52(6)	Cl(4)–Rh(1)–P(2)	92.60(6)
P(1)–Rh(1)–P(2)	178.05(6)		

$RhCl_4(PEt_3)_2]$. Thus, the addition of 2 equiv of triethylphosphine to $[PPh_4][1,6,8\text{-}Rh_2Cl_7(PEt_3)_3]$ gives stereospecifically only one isomer of each of the rhodium(III) mononuclear compounds.

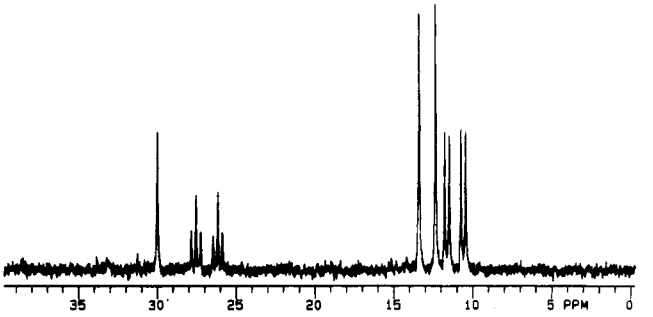

Figure 7. $^{31}P\{^1H\}$ NMR spectrum of $[PPh_4][1,6,8\text{-}Rh_2Cl_7(PEt_3)_3$ + $2PEt_3$.

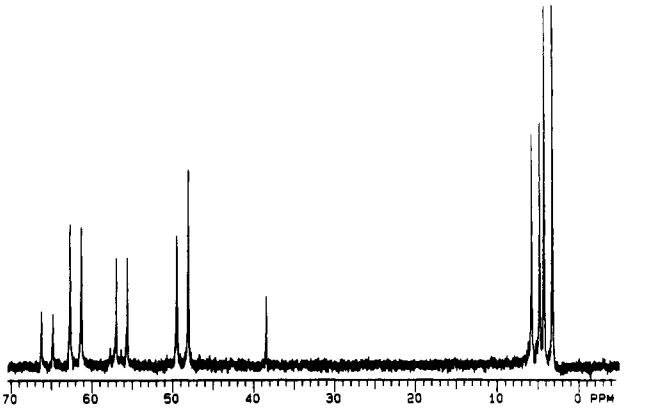

Figure 8. Disproportionation (in CH_2Cl_2) of $[1,6,8\text{-}Rh_2Br_7(PEt_3)_3]^-$ following its formation from the reaction of $[1,5\text{-}Rh_2Br_7(PEt_3)_2]^-$ with 1 molar equiv of PEt_3.

The addition of 1 equiv of trimethylphosphine to $[PPh_4][1,5\text{-}Rh_2Br_7(PEt_3)_2]$ in acetone at –40 °C led to one doublet at 55.5 ppm and a quartet of doublets centered at 1 ppm in a 1:2 ratio. The spectrum is very similar to that shown in Figure 6. The downfield doublet at 55.5 ppm (J_{Rh-P} = 114 Hz) comes from the Rh–P coupling trans to bromine whereas a quartet of doublets corresponds to two distinct phosphines mutually trans. One again, the characteristics of the $^{31}P\{^1H\}$ NMR spectrum following phosphine addition to **3b** show that the reaction of 1 equiv of trimethylphosphine with $[PPh_4][1,5\text{-}Rh_2Br_7(PEt_3)_2]$ affords stereospecifically only one edge-sharing $[PPh_4][1,6,8\text{-}Rh_2Br_7(PEt_3)_2(PMe_3)]$ isomer out of a possible eight. Upon treatment of 1 equiv of dimethylphenylphosphine, a solution of $[PPh_4][1,5\text{-}Rh_2Br_7(PEt_3)_2]$ is again converted exclusively to one isomer. The Rh–P coupling of downfield doublet at 55.7 ppm is 115 Hz, and that of four doublets centered at 2 ppm is 82 Hz.

A solution of $[NEt_4][1,5\text{-}Rh_2Br_7(PEt_3)_2]$ at CH_2Cl_2 to which one equivalent of PEt_3 has been added at –20 °C gives the spectrum shown in Figure 8. This surprisingly complex spectrum can be accounted for by the equilibrium in eq 3. The doublets at δ 56.3

$$3[1,6,8\text{-}Rh_2Br_7(PEt_3)_3]^- = [1,5\text{-}Rh_2Br_7(PEt_3)_2]^- + 1,2,6\text{-}Rh_2Br_6(PEt_3)_3 + 2[t\text{-}RhBr_4(PEt_3)_2]^- \quad (3)$$

and 5.3 (1:2) are due to the $[1,6,8\text{-}Rh_2Br_7(PEt_3)_3]^-$ ion that is initially formed by attack of PEt_3 on $[1,5\text{-}Rh_2Br_7(PEt_3)_2]^-$. The remaining doublets are all in the correct ratios to correspond to the right hand side of eq 3 when assigned as follows: $[1,5\text{-}Rh_2Br_7(PEt_3)_2]^-$, δ 62; $1,2,6\text{-}Rh_2Br_6(PEt_3)_3$, δ 65.5 and 48.7; $[t\text{-}RhBr_4(PEt_3)_2]^-$, δ 3.8.

Discussion

The studies reported here show that the previously[2] observed proclivity of halophosphino complexes of rhodium(III) to react with perfect stereo- and regiospecificity is not limited to the few

reactions already reported. It appears that such stereospecificity prevails for all such chemistry.

When reactions leading to the formation of $[Rh_2X_7(PEt_3)_2]^-$ ions are carried out in the presence of the cations $[NEt_4]^+$ and $[PPh_4]^+$ the only isolated products are those containing the $[1,5\text{-}Rh_2X_7(PEt_3)_2]^-$ anions. Moreover, at and below room temperature, these show no tendency to isomerize to the other (1,4) isomer. This result is highly reminiscent to our previous observation[1,2] that for the $Rh_2X_6(PR_3)_3$ molecules, only the 1,2,6-isomers were obtained in the preparative reaction and they showed no tendency to isomerize to the 1,2,4-isomers. It was noted then that the isomer actually obtained was the one that did not weaken (by the trans effect) both Rh–(μ-X) bonds formed by any one μ-X group, whereas the other isomer would have done so. The same point can be made with respect to the $[Rh_2X_7(PEt_3)_2]^-$ ions. We recognize, of course, that while this is a valid correlation, it does not explicitly show why the isomers obtained should have overall greater stability than the ones that were not found. Indeed, if we assume that our failure to observe any NMR signal attributable to the second isomer means that it could not have been present to the extent of more than one 50th the extent of the one seen, we can say that the $\Delta G°$ ($\approx\Delta H°$) for conversion of the observed isomer to the unobserved one (at equilibrium) would have to be $\geq$10 kJ. Since this is a rather small energy, it is possible that the two isomers could in fact differ enough in stability that one would be undetectable at equilibrium.

It is important to note that while, as explained previously,[2] $^{31}P\{^1H\}$ NMR spectroscopy has several powerful advantages in the study of this chemistry, there is also one regrettable disadvantage. Since there is no coupling between phosphorus atoms in the dinuclear species, one cannot directly tell how those on one metal atom are oriented relative to those on the other one. Specifically, in the case of a $[Rh_2X_7(PR_3)_3]^-$ ion, while it is clear that the two PR_3 ligands on one rhodium atom are trans to each other, there is no certain indication from the NMR spectrum as to whether the single PR_3 ligand on the other one is in an axial or an equatorial position. Thus, while the NMR data showed that the reaction of a $[1,5\text{-}Rh_2X_7(PR_3)_2]^-$ ion with 1 molar equiv of PR'_3 proceeds to give a unique product in which PR'_3 and one PR_3 are trans to each other in axial positions on one rhodium atom, the question of whether the other PR_3 was placed so as to give a 1,6,8- or a 2,6,8-isomer was unresolved. However, the X-ray crystal structure of $[PPh_4][1,6,8\text{-}Rh_2Cl_7(PEt_3)_2(PMe_3)]$ (**2**) resolved this ambiguity.[8]

The behavior of the $[Rh_2Br_7(PEt_3)_2]^- + PEt_3$ system is particularly interesting since it shows that this system (and presumably all others, in principle) are able to evolve toward the appropriate mixture of species, as shown in eq 3, but that only one isomer of each is present. It may, of course, be true that this is a thermodynamically dictated result, each observed isomer being that only one that is thermodynamically stable. However, the observed result could also have a purely mechanistic explanation, such that once one component was restricted to only one isomeric form, it might be mechanistically impossible to break out of one reaction scheme. Indeed, it is also possible to attribute the failure of other isomers to show up in solutions where only one type of compound is detected to purely mechanistic causes.

Acknowledgment. We thank the National Science Foundation for support.

Supplementary Material Available: Full tables of crystallographic data, anisotropic thermal parameters, and molecular dimensions (50 pages). Ordering information is given on any current masthead page.

(8) There is a possibility that for the 2,6,8-isomer, the chemical shifts of the 6- and 8-PR_3 groups would differ because of the influence of the 2-PR_3 group on the 6-PR_3 group. Rigorously, the 6- and 8-PR_3 groups are not equivalent. However, the magnitude of such an effect is impossible to estimate but likely to be small. It would be unsafe to rule out the possibility of the 2,6,8-isomer just because no indication of such an influence is detected.